THE EFFECT OF THE STRUCTURAL PROPERTIES ON THE SEY OF C MATERIALS.

L. A. Gonzalez, M. Angelucci, R. Larciprete[1] and R. Cimino LNF-INFN, 00044 Frascati (Roma), Italy
[1]also at CNR-ISC Istituto dei Sistemi Complessi, 00185 Roma, Italy.

Abstract

We review here the dependence of the secondary electron yield (SEY) of carbon materials on the structural ordering of the C lattice and surface damage. We followed the SEY evolution during the thermal graphitization of thin amorphous carbon layers and during the amorphization of highly oriented pyrolytic graphite by means of Ar^+ bombardment. C1s core level and valence band spectroscopy, used to follow the structural modification, were measured in parallel with SEY curves. In the first case the SEY decrease observed with the progressive conversion of sp^3 hybrids into six-fold aromatic domains was related to the electronic structure of the C-films close to the Fermi level. We found that a moderate structural quality of the C layer, corresponding to aromatic clusters of limited size, is sufficient to obtain a SEY as low as ~ 1. For the bombarded graphite, the strong lattice damaging remains limited to the near surface layer, where the high density of defects reduces the transport of incoming and secondary electrons. Then, the SEY curves resulted differently modified in the low and high primary energy regions, but their maximum values remained favorably low. Our findings demonstrate that SEY, besides being an indispensable means to qualify technical materials in many technological fields, can be also used as a flexible and advantageous diagnostics to probe surfaces and interfaces.

INTRODUCTION

Secondary Electron Yield (SEY) is an ubiquitous property of matter determining the actual behavior of a surface in a device and/or in technologically relevant applications. In general, an efficient SEY reduction for materials exposed to high radiation doses might rely on the use of specific low emitting coatings, especially based on C, as it has been recently proposed for the baseline design of the high luminosity large hadron collider (HL-LHC) [1] and, potentially, for future circular colliders (FCC-hh) [2]. The beneficial effect of carbon coatings is usually related to the moderate SEY of the sp^2 C hybridization, lower with respect to other hybridization states [3], as it has been ascertained for several nanographitic materials as fullerene [4], nanotubes [5], graphene [6, 7] and graphene nanoplatelets [8]. The relevance of this issue makes the knowledge of the relation between microstructural and electronic properties of C materials and their macroscopic SEY highly desirable. On the other hand, C layers deposited on large areas, with techniques compatible with the geometry of accelerator components, may lack of high structural quality. Furthermore, even good graphitic layers, once exposed to electron, photon and ion fluxes during machine operation, might result severely damaged. It is therefore important to validate the SEY properties of graphitic films while their structural quality is altered by external factors.

In order to shed light on these points, in the last years we investigated the effect that the structural ordering of the C lattice has on the macroscopic SEY properties of ultrathin C layers. To this aim in a first study [9] we deposited amorphous C films on copper substrates and used x-ray (XPS) and ultraviolet (UPS) photoelectron spectroscopy to follow *in situ* the $sp^3 \rightarrow sp^2$ structural reorganization and the coalescence of the sp^2 clusters into nanocrystalline graphite induced by thermal annealing, while probing in parallel the SEY properties of the samples. In order to explore the opposite process, in a second study [10] we introduced controlled densities of crystal defects in a highly oriented pyrolytic graphite (HOPG) sample by subsequent cycles of Ar^+ ion bombardment at low kinetic energy (500 eV). Also in this case the effects of the lattice defects on the electronic, structural and secondary emission properties were monitored by measuring *in situ* UPS and XPS spectra together with SEY curves. Special attention was paid not only to the variation of the maximal SEY value, but also to more subtle changes on the entire curve, with a particular attention to the low energy secondary electron yield LE-SEY at low (<40 eV) primary electron energy [11]. In the following we summarize the results and elucidate the discordant behavior observed for the two systems.

EXPERIMENTAL

The experiments were performed in the Material Science Laboratory of the INFN-LNF at Frascati (Rome, Italy), in an ultra-high vacuum (UHV) system consisting of a preparation chamber and an analysis chamber, both having a base pressure of $2–5\times10^{-10}$ mbar.

Carbon films were grown on polycrystalline Cu substrates at room temperature by radiofrequency magnetron sputtering using a power of 50 W and Ar pressure of 6×10^{-2} mbar. The thickness of the films used for this experiment was estimated to be of the order of 20 nm. Thermal annealing was performed in steps, by heating for 30 minutes the sample at a fixed temperature up to 1070 K. The temperature was measured by a calibrated pyrometer.

The HOPG sample was cleaved with adhesive tape before being loaded into the UHV system. Prolonged thermal annealing at temperatures of $\sim$ 1000 K was carried out to desorb contaminants, whose absence was crosschecked by XPS. The HOPG was Ar^+ ion bombarded at 500 eV and Ar pressure of 5×10^{-6} mbar for increasing doses up to $4.5\times10^{14} \pm 0.1$ Ar^+/cm^2. After each ion dose, UPS and XPS analysis

of the surface, as well as SEY measurements were carried out.

XPS and UPS measurements were performed by using an Omicron EA125 analyzer to reveal the photoelectrons excited by the non monochromatic radiation of Al Kα (hν = 1486.7 eV) or Mg Kα (hν = 1254.6 eV) and He II (hν =40.8 eV) sources, respectively.

The SEY(δ) is defined as $SEY=I_{out}/I_p=(I_p-I_s)/I_p$, where I_p is the current of the primary electron beam hitting the sample, I_{out} is the current of the electrons emerging from the sample and I_s is the sample current to ground, as measured by a precision amperometer. SEY is measured as described in detail in Refs. [12, 13]. In brief I_p (some tens of nA) was measured by means of a Faraday cup positively biased, whereas I_s was determined by biasing the sample at -75 V. SEY curves as a function of the primary energy E_p are characterized by a maximum value (δ_{max}) reached in correspondence of a certain energy (E_{max}).

RESULTS AND DISCUSSION

In the first study [9] we deposited amorphous C films on copper substrates and followed *in situ* the $sp^3 \rightarrow sp^2$ structural reorganization induced by thermal annealing , while acquiring at each step the SEY curve . Figures 1a and 1b show the evolution of the C1s and valence band spectra. The C1s spectrum measured on the as-deposited a-C layer (upper curve in Fig.1a) is peaked at 284.65 eV and exhibits a FWHM of 1.8 eV. The shift of 0.35 eV with respect to the position of the graphitic carbon indicates the presence a consistent fraction of sp^3 hybridized atoms. Accordingly, the valence band measured on the as-deposited layer (top curve in Fig.1b) shows only a broad unstructured peak centered at 7.7 eV related to the σ bonds, consistent with the presence of sp^2 chains and limited aromatic domains coexisting with the sp^3 phase. In the Fermi level region the VB spectrum reveals the presence of an energy gap of $\sim$ 0.4 eV. With thermal annealing, the main σ peak progressively narrows and the feature related to the π band in graphite appears at $\sim$ 3 eV, indicating a rising concentration of the six-fold coordinated rings. In parallel, the density of states in the region close to the Fermi level increases and in the sample annealed at 1070 K resembles the quasi metallic character typical of the graphitic structures. Also the C1s peak manifests the occurrence of graphitization. The BE of C1s photoelectrons in C materials is related to the hybridization state of the emitting atoms and is a useful mean to estimate the sp^3/sp^2 ratio, since typically the sp^3 and sp^2 fingerprint components are found with a separation of 0.8-0.9 eV [14]. The spectra in Fig.1a show that, with increasing annealing temperature, the C1s peak shifts to lower BE due to the progressive decrease of the sp^3 component, and after the annealing at 1070 K is peaked at 284.3 eV. However, even if this change indicates a substantial $sp^3 \rightarrow sp^2$ conversion, the wide spectral FWHM of the C1s peak (1.5 eV) reveals a low structural quality of the sp^2 network. The evolution of the SEY and LE-SEY curves with thermal annealing is summarized in Figs.2a and 2b. The slight δ_{max} decrease from 1.25 to 1.16 induced by the annealing to 710 K is followed by a more substantial reduction to 1.03 for the film annealed at 900 K, whereas after the last annealing step δ_{max} decreases to 0.99 and E_{max} shifts to 250 eV. The same trend indicating the SEY reduction is evident in the low energy region (Fig.2a).

Among the factors that might be at the origin of the observed behavior we can disregard the variation of the work function, which for nanographitic C has been shown to decrease with graphitization [15], and would then correspond to an increase of SEY. Instead, the behavior in the vicinity of the Fermi level can play a role. In a-C the presence of a gap at the Fermi level, setting a prohibited energy interval, reduces the probability for secondary electrons to lose energy through electron-electron collisions [4]. With the expansion of the graphitic domains induced by thermal annealing, the disappearance of the energy gap and the increasing number of electronic states close to the Fermi level likely raise the energy dissipation channels and reduce the diffusion length, thus effectively contributing to lower the yield of the secondary electrons emerging from the sample surface. Then the decrease in the SEY is directly related to the extent of graphitization. It is worth noting that Raman spectroscopy (not shown) has established that the average dimension of the graphitic crystallites, which is of the order of 1.3 nm in the pristine a-C layer, after annealing does not exceed $\sim$ 3.8 nm, confirming the moderate crystalline quality of the annealed film indicated by the width of the C1s peak. Then, it turns out that the presence or aromatic clusters of a few nanometers in size is sufficient to lower the macroscopic SEY to the level of graphitic carbon with much higher structural ordering [9]. It is likely that in materials with small graphitic grains the enhanced scattering at the grain boundaries provides an additional contribution to reduce the number of secondary electrons emerging from the surface.

In the second part of this study we started with a HOPG sample and introduced controlled amounts of defects in the crystalline lattice by subsequent cycles of Ar^+ ion bombardment at low kinetic energy (500 eV). Low energy ion bombardment can produce interstitial defects created by trapping incident ions underneath the carbon planes and generate vacancies in the graphitic network. The structural defects are expected to change the electronic and structural properties of HOPG and consequently to affect its secondary emission properties.

The extent of Ar^+ induced HOPG amorphization was monitored by C1s and valence band spectroscopy. Figure 1c shows that the C1s peak, which for HOPG is located at BE of 284.2 eV, after Ar^+ bombardment remains centered at the same BE and exhibits a broader line shape. Hence, ion bombardment ruins the crystalline network without inducing a real change in the hybridization of the C atoms. Similar indications are provided by the valence band spectra shown in Fig.1d. The spectrum of the intact HOPG exhibits sharp features at 4.3 (σ band) and 7.5 eV (π band) [16] (the peak

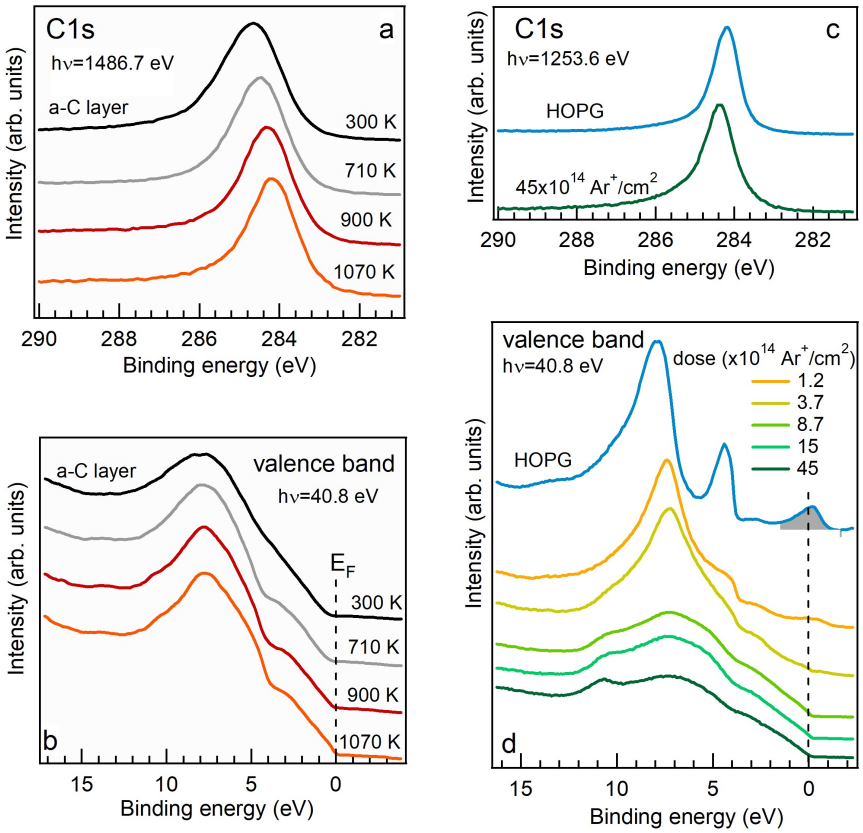

Figure 1: a) C1s and b) valence band spectra measured on the as-prepared a-C layer (black curves) and as function of the annealing temperature. c) C1s and d) valence band spectra measured on the pristine HOPG sample and after the exposure to increasing doses of Ar^+ ions with kinetic energy of 500 eV.

just above the Fermi Level is related to photoelectron emission excited by the He II satellite at hν=48.4 eV). Both bands progressively weaken and the broad unstructured features observed for doses higher than 5.0×10^{13} Ar^+/cm^2 reveal a total amorphization of the crystalline structure. The indications provided by the valence band spectra are paralleled by the evolution of the LE-SEY curves measured as a function of the ion dose (Fig.2d). The curve measured on pristine HOPG shows features related to the elastic and inelastic electron-solid interactions, which provide direct information on the unoccupied band structure [17, 18]. Such structured line shape is progressively canceled as the ion dose increases, due to the loss of crystalline ordering after the nucleation of lattice defects. At dose of 1.5×10^{14} Ar^+/cm^2 the smooth curve profile is clearly indicative for the presence of strong disorder in the probed sample depth. Complementary information is provided by the extended SEY curves shown in Fig.2e. The intact HOPG exhibits a maximum value of 1.0 for E_p in the 220-400 eV range. With rising ion dose, for $E_p > 200$ eV the SEY progressively decreases up to the ultimate value of 0.6. On the other hand in the low E_p region, δ_{max} rises to 1.1 for doses of the order of 15×10^{13} Ar^+/cm^2. We can then conclude that graphite maintains favorable secondary emission properties even when significantly defected. However the contrasting SEY behavior, which with increasing lattice defectivity rises at low E_p and decreases at high E_p, deserves a clarification.

It is interesting to compare this trend to the behavior observed in the previous paragraph during the graphitization of the a-C films. As can be seen in Figs.2b and 2e, whereas in the first case thermal annealing determines a nearly constant SEY reduction in the whole E_p region, ion bombardment modifies selectively the SEY of HOPG. The discordant behavior is made more evident by plotting in Fig.2c the δ_{max} values vs. annealing temperature measured for the first experiment, which show a trend consistent with the homogeneous graphitization of the whole layer, and in Fig.2f the SEY values measured at E_p=175 and 800 eV in the second experiment, showing at high, but not at low E_p, the SEY drop with increasing sputtering dose.

In order to explain the observed results one must consider that the localized states which appear near the defect sites act as scattering centers for electron waves, which affect the transport properties of the damaged HOPG surface layer, decreasing the electron mean free path with respect to defect-free lattice. The ion bombardment produces a "bi-layered" structure, with a ~2 nm thick damaged layer [10] on top of the pristine HOPG bulk. Consequently, the transport of

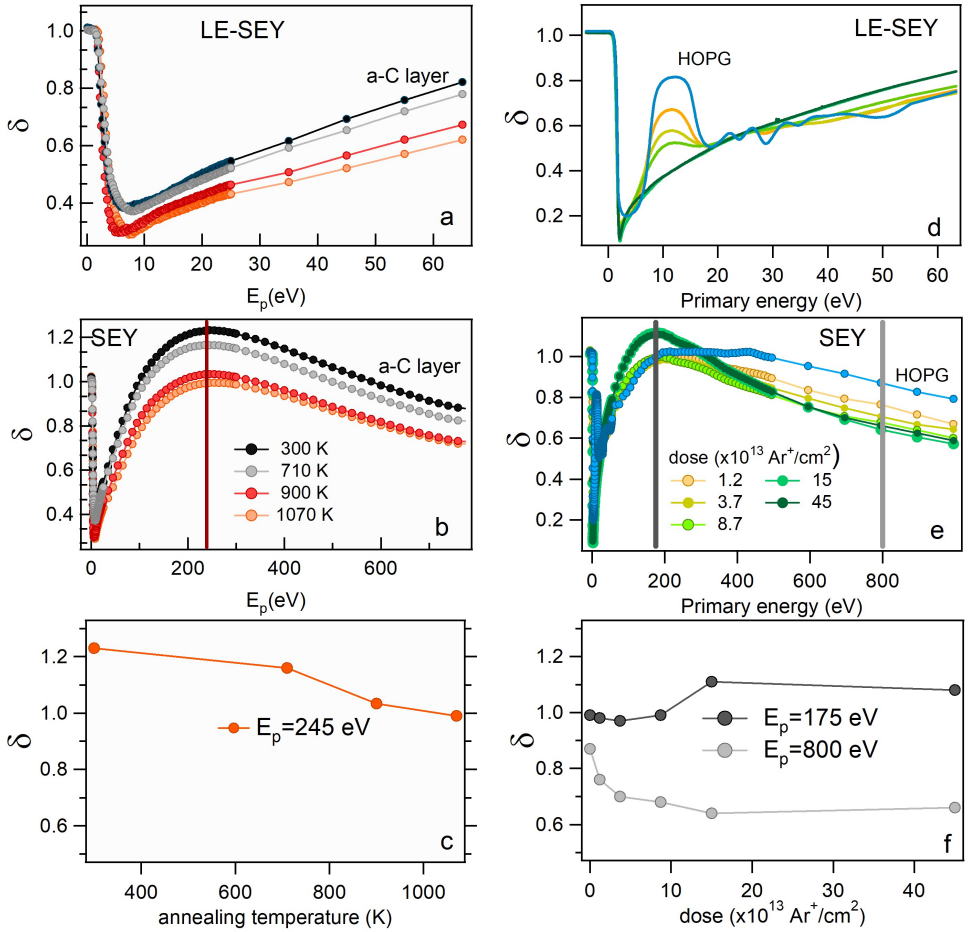

Figure 2: a) LE-SEY and b) SEY curves measured on the as-prepared a-C layer (black curves) and as function of the annealing temperature. d) LE-SEY and e) SEY curves measured on the pristine HOPG sample and after the exposure to increasing doses of Ar^+ ions with kinetic energy of 500 eV. c) δ_{max} values (E_p=245 eV) vs. annealing temperature measured during the graphitization of the a-C films (cfr. Fig.2b); f) δ values measured at E_p=175 and 800 eV vs. the Ar^+ dose during the amorphization of HOPG (cfr. Fig.2e).

primary and secondary electrons depends on whether they move through the defected or through the intact graphitic lattice [10]. The primary electron penetration depth λ, which for 40 eV $\geq E_p \geq$ 200 eV is $\leq$ 1 nm [19], decreases in the presence of defects, which means which *i)* primary electrons penetrate less than in the case of crystalline HOPG and *ii)* secondary electrons are produced in regions closer to the surface and escape more effectively to vacuum. Such effects finally determine the observed increase of SEY at Ep=200 eV after very high Ar^+ doses. At E_p=800 eV the kinetic energy of the primary electrons is sufficiently high that they will cross the damaged surface barrier. In that case the secondary electrons generated within the undamaged underlying HOPG, when traveling towards the surface with kinetic energies below 50 eV, suffer a significant mobility reduction [20], which hampers their escape into vacuum. This effect becomes more significant with increasing defect density at high ion doses.

CONCLUSIONS

We have shown that for C materials the SEY behavior and the structural properties are closely related. For amorphous C thin films the secondary emission decreases with the conversion of sp^3 hybrids to six-fold aromatic domains and the reason of that has been identified in the strong correlation between the electronic structure close to the Fermi level and the yield of secondary electrons. What is relevant is that a moderate structural quality of the C layer is sufficient for a considerable SEY decrease as aromatic clusters of limited size approach the secondary emission properties of graphite.

Amorphization of HOPG has been proved to modify the SEY curve, whose δ_{max}, however, remains stable and low ($\leq$1.1) even in the presence of a high defect density. The resulting LE-SEY curves strongly depend on the lattice ordering, which may have significant implications on simulations where SEY and LE-SEY curves are parametrized.

In conclusion we can remark that SEY and LE-SEY are valid tools, which, with a limited experimental requirement,

can be used as flexible diagnostics sensitive to chemical and structural properties of materials.

ACKNOWLEDGEMENTS

This work was supported by LNF through the grV project "MICA" . The authors wish to thank the DAFNE-L technical team for continuous assistance during the experiments.

REFERENCES

[1] G. Apollinari and I. Béjar–Alonso and O. Brüning and P. Fessia and M. Lamont and L. Rossi and L. Tavian, *High Luminosity Large Hadron Collider (HL-LHC): Technical Design Report V.0.1*, CERN Yellow Reports: Monographs; 4/2017

[2] R. Cimino, V. Baglin, and F. Schäfers, Phys. Rev. Lett. 115, 264804 (2015)

[3] M. Nishiwaki and S. Kato, J. Vac. Soc. Jap. 118, 48 (2005)

[4] J. M. Ripalda, I. Montero, L. Vázquez, D. Raboso, and L. Galán, J. Appl. Phys. 99, 043513 (2006)

[5] M. K. Alam, P. Yaghoobi, M. Chang, and A. Nojeha, Appl.Phys. Lett. 97, 261902 (2010)

[6] J. Luo, P. Tian, C.T. Pan, A. W. Robertson, J. H. Warner, E. W. Hill, and G. A. D. Brigg, ACS Nano 5, 1047 (2011)

[7] H. Hiura, H. Miyazaki, and K. Tsukagoshi, Appl. Phys. Expr. 3, 095101 (2010)

[8] I. Montero, L. Aguilera, M. E. Davila, V. C. Nistor, L. A. Gonzalez, L. Galan, D. Raboso, and R. Ferritto, Appl. Surf. Sci. 291, 74 (2014)

[9] R. Larciprete, D. Grosso, A. D. Trolio, and R. Cimino, App. Surf. Sci. 328, 356 (2015)

[10] L. Gonzalez, R. Larciprete, and R. Cimino, AIP Advances 6, 095117 (2016)

[11] R. Cimino, L. Gonzalez, R. Larciprete, A. Di Gaspare, G. Iadarola, and G. Rumolo, Phys. Rev. ST Accel. Beams 18, 051002 (2015)

[12] R. Larciprete, D. Grosso, M. Commisso, R. Flammini, and R. Cimino, Phys. Rev. ST Accel. Beams 16, 011002 (2013)

[13] R. Cimino and T. Demma, Int. J. Mod. Phys. A 29, 1430023 (2014)

[14] J. Diaz, G. Paolicelli, S. Ferrer, and F. Comin, Phys. Rev. B 54, 8064 (1996)

[15] A. Ilie, A. C. Ferrari, T. Yagi, S. E. Rodi, J. Robertson, E. Barborini, and P. Milani, J. Appl. Phys. 90, 2024 (2001)

[16] S. Y. Zhou, G.-H. Gweon, C. D. Spataru, J. Graf, D.H. Lee, S. G. Louie, and A. Lanzara, Phys. Rev. B 71, 161403 (2005)

[17] P. J. Mølert and M. H. Mohamed, J. Phys. C: Solid State Phys. 15, 6457 (1982)

[18] R. F. Willis, B. Fitton, and G. S. Painter, Phys. Rev. B 9, 1926 (1974)

[19] M. P. Seah and W. A. Dench, Surf. Interf. Analysis 1, 1 (1979).

[20] A. Lherbier, B. Biel, Y.-M. Niquet, and S. Roche, Phys. Rev. Lett. 100, 036803 (2008)